Insulin Receptor Isoform A and Insulin-like Growth Factor II as Additional Treatment Targets in Human Osteosarcoma

Sofia Avnet,[1,3] Laura Sciacca,[4] Manuela Salerno,[1] Giovanni Gancitano,[1] Maria Francesca Cassarino,[4] Alessandra Longhi,[2] Mahvash Zakikhani,[5] Joan M. Carboni,[6] Marco Gottardis,[6] Armando Giunti,[1,3] Michael Pollak,[5] Riccardo Vigneri,[4] and Nicola Baldini[1,3]

[1]Laboratory for Pathophysiology and [2]Chemotherapy Unit, Rizzoli Orthopaedic Institute, and [3]Department of Human Anatomy and Musculoskeletal Pathophysiology, Section of Orthopaedic Surgery, University of Bologna, Rizzoli Orthopaedic Institute, Bologna, Italy; [4]Department of Internal and Specialistic Medicine, Endocrinology, University of Catania, Garibaldi-Nesima Hospital, Catania, Italy; [5]Department of Oncology, McGill University, Montreal, Quebec, Canada; and [6]Oncology Drug Discovery, Pharmaceutical Research Institute, Bristol-Myers Squibb Co., Princeton, New Jersey

Abstract

Despite the frequent presence of an insulin-like growth factor I receptor (IGFIR)-mediated autocrine loop in osteosarcoma (OS), interfering with this target was only moderately effective in preclinical studies. Here, we considered other members of the IGF system that might be involved in the molecular pathology of OS. We found that, among 45 patients with OS, IGF-I and IGFBP-3 serum levels were significantly lower, and IGF-II serum levels significantly higher, than healthy controls. Increased IGF-II values were associated with a decreased disease-free survival. After tumor removal, both IGF-I and IGF-II levels returned to normal values. In 23 of 45 patients, we obtained tissue specimens and found that all expressed high mRNA level of IGF-II and >IGF-I. Also, isoform A of the insulin receptor (IR-A) was expressed at high level in addition to IGFIR and IR-A/IGFIR hybrids receptors (HR^A). These receptors were also expressed in OS cell lines, and simultaneous impairment of IGFIR, IR, and Hybrid-Rs by monoclonal antibodies, siRNA, or the tyrosine kinase inhibitor BMS-536924, which blocks both IGFIR and IR, was more effective than selective anti-IGFIR strategies. Also, anti–IGF-II-siRNA treatment in low-serum conditions significantly inhibited MG-63 OS cells that have an autocrine circuit for IGF-II. In summary, IGF-II rather than IGF-I is the predominant growth factor produced by OS cells, and three different receptors (IR-A, HR^A, and IGFIR) act complementarily for an IGF-II–mediated constitutive autocrine loop, in addition to the previously shown IGFIR/IGF-I circuit. Cotargeting IGFIR and IR-A is more effective than targeting IGF-IR alone in inhibiting OS growth. [Cancer Res 2009;69(6):2443–52]

Introduction

Although combination treatments have significantly improved the prognosis of osteosarcoma (OS; ref. 1), the survival rate has now reached a plateau (2, 3), and further improvements may only derive from a better understanding of molecular pathology (4–7), particularly mechanisms underlying bone growth and remodeling. In fact, the peak incidence of OS coincides with adolescent growth spurt, and the observed association between OS and height (8–10) suggests the importance of growth factors and receptors involved in skeletal growth (11). Among these, insulin-like growth factor I (IGF-I) also promotes the initiation and progression of many malignancies, including sarcomas (12, 13). The IGF-I/IGFIR autocrine circuit is relevant for OS growth, *in vitro* (14, 15), and in clinical settings (16, 17), although therapies against IGFIR have only resulted in a limited beneficial effect (5, 18). Less attention has been paid to the other cognate stimulator of the IGF signaling pathway, IGF-II. Under physiologic conditions, IGF-II is abundantly stored in the bone matrix (19), and during fetal development, IGF-II expression is higher than in the postnatal life (20). In most tissues, IGF-II is maternally imprinted (21), but this imprinting is usually lost in cancer (22, 23), leading to IGF-II biallelic production that provides an increased growth-promoting signaling. IGF-II mRNA is expressed by human OS cell lines and tissues (11, 16, 18), and IGF-II loss of imprinting has been shown in OS (24).

Although IGF-I and IGF-II both interact the same receptor, IGFIR, IGF-II can also bind with high affinity to the isoform A of insulin receptor, IR-A. IR-A is generally expressed at lower levels than IR-B, although this is not the case in fetal and cancer cells (25). An autocrine loop mediated by IR-A/IGF-II is present in leiomyosarcoma (26), where it is crucial for cell proliferation and migration.

Both IR and IGFIR are tetrameric complexes consisting of two identical extracellular α-subunits that bind insulin, and two identical β-subunits that have tyrosine kinase activity. In cells and tissues coexpressing both IR and IGFIR, hybrid-receptors (HR) can be formed by one α-and oneβ-subunit IR heterodimer, and one α-and one β-subunit IGFIR heterodimer (27, 28). The affinity of IGF-I and IGF-II for these HR is still unclear (29); however, all tissues expressing IR and IGF-IR also express HR, leading to an additional IGF/HR circuit.

In this study, we evaluated the serum levels of IGF-I and IGF-II in OS patients, and the expression of IR, IGF-IR, and HR in OS specimens. We also compared the effects of different strategies aimed at inhibiting IGF-II, or IGFIR, or both IR and IGFIR. Our findings indicate that, in addition to the IGFIR/IGF-I autocrine loop, other circuits, mediated by IR-A and HR, are activated by IGF-II and are relevant for the molecular pathology of OS.

Materials and Methods

Reagents. The reagents purchased were as follows: IMDM, and penicillin, streptomycin (Invitrogen); protease-inhibitor cocktail (Roche); Bradford assay and SDS sample buffer (Bio-Rad); TRIzol reagent (Invitrogen); Advantage RT-for-PCR kit (Clontech); IGF-I and IGF-II (Calbiochem); BMS-536924 (Bristol Myers); Protein-G-plus-agarose beads and anti-αtubulin B7

Requests for reprints: Sofia Avnet, Istituto Ortopedico Rizzoli, via di Barbiano 1/10, 40136 Bologna, Italy. Phone: 39-051-636678; Fax: 39-051-6366748; E-mail: sofia.avnet@ior.it.

doi:10.1158/0008-5472.CAN-08-2645

monoclonal antibody (MAb; Santa Cruz Biotechnology), LiteAblot (Euroclone); Restore Western Blot Stripping buffer (Pierce); horseradish peroxidase–conjugated anti-rabbit or anti-mouse antibodies (Amersham); FITC-coniugated anti-rabbit polyclonal antibody (Dako); SeaPlaque Agarose (FMC BioProducts); anti–IGFIR-siRNA (Silence Therapeutics); anti–IR-siRNA and anti–IGF-II-siRNA (Dharmacon); anti–Phospho-44/42 MAP kinase, anti-p44/42 MAP kinase, and anti–Phospho– insulin receptor substrate-1 (IRS-1) polyclonal antibodies (Cell Signaling); anti–phospho-IGFIR/IR JY202 MAb, anti–IRS-1 polyclonal antibody, and S1F2 anti–IGF-II MAb (Upstate); MPOC-21 isotype control MAb (Becton Dickinson); porcine insulin, and all other reagents from Sigma.

Primary antibodies against (*a*) anti-IGFIR: αIR-3 MAb (Oncogene Research), 17-69 MAb obtained as described (27) and C-20 polyclonal antibody (Santa Cruz Biotechnology); and against (*b*) anti-IR: MA-20 MAb, CT-1 MAb, 83-7 MAb obtained as described (27), 83-14 MAb (Biomeda), and a polyclonal rabbit antibody (Becton Dickinson).

Subjects and sample collection. Fifty-three patients with newly diagnosed high-grade OS were seen at our institution from May 2002 through July 2005, signed informed consent regarding the use of their biological materials for research studies, and entered the study. At presentation, seven patients had detectable pulmonary metastases and four multiple localizations. Blood and tumor tissues were collected after the institutional ethical committee approval.

Serum samples were obtained from 45 of 53 patients (33 males and 12 females; age, 13 ± 1 y) before treatment and from 17 age-paired healthy controls (8 males and 9 females; age, 12 ± 1 y). In 9 patients, serum was also collected 12 mo since diagnosis, after treatment completion. Tissue specimens were collected from 23 OS untreated patients. In 15 cases, serum and biopsy samples were available from the same individuals. Hence, the 53 patients were subdivided in 3 subgroups, depending on the availability of biological materials: (*a*) subgroup A (n = 45), patients in which serum samples were available; (*b*) subgroup B (n = 35), a fraction of patients of subgroup A, characterized by the absence of metastases at presentation; and (*c*) subgroup C (n = 23), patients in which tissue specimens were retrieved (Table 1). The median follow-up of patients of subgroup B, treated by surgery plus multiagent chemotherapy (30), was 54 mo (minimum 34 mo). Adverse events were defined as tumor recurrence at any site or death during remission. The event-free survival duration was calculated from the date of diagnosis. Results were updated in February 2008: 24 patients (68.6%) were disease free, 9 (25.7%) had metastases, and 2 (5.7%) had both local recurrence and metastases.

Cell lines. Saos-2 and MG-63 human OS cell lines, purchased from the American Type Culture Collection, were cultured in IMDM plus 20 units/mL penicillin, 100 μg/mL streptomycin, 10% FCS (complete medium), and incubated at 37°C in a humidified 5% CO_2 atmosphere.

IGF-I, IGF-II, and IGFBP-3 measurement. Serum levels or protein content in the cell lysates of IGF-I, IGF-II, and IGFBP-3 were measured by ELISA (Diagnostic Systems Laboratory). Protein lysates were obtained using radioimmunoprecipitation assay buffer [RIPA; 0.05 mol/L Tris-HCl (pH 7.4), 150 mmol/L NaCl, 5% Triton X-100, 1 mmol/L EGTA, 1 mmol/L NaF] from semiconfluent cells. Protein content was measured by the Bradford assay.

IGFIR, IR, and HR in tissue specimens and cell lines. IGFIR, IR, and HR were measured by ELISA as described (27). Frozen tissues were pulverized in the presence of liquid nitrogen. Powdered tissues or subconfluent cell monolayers were solubilized with RIPA buffer supplemented with complete protease inhibitor cocktail, phenylmethylsulfonyl fluoride 1 mmol/L, and Na_3VO_4 0.2 mmol/L. Protein content was measured by the Bradford assay.

To immunocapture different receptors, specific MAb that do not cross-react with other receptors were used (27) as follows: against IR, MA-20; against IGFIR, αIR-3; and against HR, 83-7. Th secondary MAb used were as follows: against IR, CT-1 biotinylated; against IGFIR, 17-69 biotinylated; and against HR, 17-69 biotinylated.

Isolation of mRNA and reverse transcription-PCR. Messenger RNA from powdered tissues or from semiconfluent cells was extracted using TRIzol reagent. Total RNA was reverse transcribed into cDNA using the Advantage RT-for-PCR kit. Reverse transcription-PCR (RT-PCR) consisted in one denaturation at 94°C for 5 min, 30 cycles of amplification (denaturation at 94°C for 30 s, annealing at the specific temperature for 30 s, and extension at 72°C for 45 s), and a final extension at 72°C for 7 min. Forward and reverse primers:

IGF-I: 5′-GATGCACACCATGTCCTCCT-3′, 5′-TCCTGCGGTGGCATGTCACT-3′
IGF-II: 5′-CTGGTGGACACCCTCCAGTTC-3′, 5′-GCCCACGGGGTATCTGGGGAA-3′
IR: 5′-AACCAGAGTGAGTATGAGGAT-3′, 5′-CCGTTCCAGAGCGAAGTGCTT-3′
β-actin: 5′-TCTGGCACCACACCTTCTACAATGAGCTGCG-3′, 5′-CGTCATACTCCTGCTTGCTGATCCACATCTGC-3′.

Products were separated by electrophoresis. A digital image was acquired by the Gel Doc XR system, and the signal intensity was quantified by Quantity One (Bio-Rad) and related to β-actin signal. RT-PCR was replicated thrice.

Cell growth after treatment with IGF-I, IGF-II, or insulin. Cells were seeded in 12-well plates (30,000 cells per well) in complete medium and, after 24 h, incubated with serum-free medium. After an additional 24 h, IGF-I, IGF-II, or porcine insulin (10 nmol/L) were added, and after 3 d, cells were counted by trypan blue. The assay was repeated thrice in duplicate.

Immunoblotting and immunoprecipitation. Immunoprecipitation was performed to detect IGFIR or IR phosphorylation, and Western blot was made to detect extracellular signal-regulated kinase (ERK) and IRS-1 phosphorylation in total lysates. For immunoprecipitation, subconfluent cells were serum-starved for 24 h and then exposed to IGF-I, IGF-II, or insulin (10 nmol/L) for 15 min. In BMS536924 assay, cells were pretreated for 1 h in serum-free medium with the drug (0.00–0.25–1.00–5.00 μmol/L), and then exposed for 15 min to IGF-II (10 nmol/L). For direct immunoblotting of total protein, cells were serum starved for 24 h and then treated for 5, 15, and 60 min with IGF-I, IGF-II, or insulin (10 nmol/L). In BMS536924 assay, cells were pretreated for 1 h in serum-free conditions with BMS536924 (0.00–0.01–0.10–0.25–0.50–1.00–2.50–5.00 μmol/L) and then incubated for 15 min with IGF-II (10 nmol/L). Protein lysates were obtained in RIPA buffer supplemented with protease inhibitors. Protein-G-plus-agarose beads were shaken with 500 μg of lysates and with αIR-3 MAb or anti–IR 83-14 MAb. The pelleted beads were resuspended in SDS sample buffer, boiled, centrifuged, and the supernatants were resolved by electrophoresis on a polyacrylamide gel. Blots were probed with C-20 anti-IGFIR or with anti-IR rabbit polyclonal antibodies, or with anti–phospho-IGFIR/IR MAb.

For Western blot analysis, equal amounts of protein lysates were subjected to reducing SDS-PAGE on a polyacrylamide gel, transferred to nitrocellulose membranes, and subjected to immunoblot analysis. Blots were probed with Phospho-44/42 MAP kinase or p44/42 MAP kinase or Phospho-IRS-1, or IRS-1 polyclonal antibodies. Incubation with a horseradish peroxidase–conjugated anti-rabbit or anti-mouse antibodies followed. To detect different antigens within the same blot, nitrocellulose membranes were stripped with Restore Western Blot Stripping buffer and reprobed. The reaction was revealed by a chemiluminescence substrate (LiteAblot). Immunoprecipitation and direct immunoblot assays were repeated thrice.

IRS-1 cell localization. Starved cells were cultured on glass coverslips for 24 h. IGF-I, IGF-II, or insulin were then added for 4 h (30–100–300 nmol/L). Cells were fixed with 3% paraformaldehyde and 300 mmol/L sucrose, and permeabilized with 0.1% Triton X-100. Coverslips were incubated with anti–IRS-1 polyclonal antibody, then with FITC-coniugated anti-rabbit polyclonal antibody in PBS containing propidium iodide (1 μg/μL) and RNase A (10 μg/mL), and observed by confocal microscopy with argon and helium-neon lasers (D-Eclipse C-1; Nikon). This assay was repeated twice. Cells with IRS-1 nuclear localization were counted in three different fields (positive cells per 100 cells).

Cell proliferation blockade. *a) Antibodies and tyrosine kinase inhibitor blocking strategies.* Cells were seeded in 12-well plates (30,000 cells per well) in complete medium. After 24 h, medium was changed with new complete medium containing αIR-3 anti-IGFIR MAb (1 μg/mL), or S1F2 anti–IGF-II

Table 1. Clinical and pathologic features of OS patients

Variable	Total Series (n = 53)	Subgroup A (n = 45)	Subgroup B (n = 35)	Subgroup C (n = 23)
Age (y)				
≤14	28 (53)	26 (58)	20 (57)	8 (35)
>14	25 (47)	19 (42)	15 (43)	15 (65)
Sex				
Male	38 (72)	33 (73)	25 (71)	16 (70)
Female	15 (28)	12 (27)	10 (29)	7 (30)
Anatomic site				
Femur	27 (51)	22 (49)	18 (51)	14 (61)
Tibia	11 (21)	10 (22)	9 (26)	5 (22)
Humerus	8 (15)	7 (16)	6 (17)	2 (9)
Pelvis	1 (2)	0	0	1 (4)
Fibula	2 (4)	2 (4)	2 (6)	0
Multiple	4 (8)	4 (9)	0	1 (4)
Histologic subtype				
Osteoblastic	36 (68)	32 (71)	24 (69)	16 (70)
Chondroblastic	9 (17)	6 (13)	4 (11)	5 (22)
Fibroblastic	4 (8)	4 (9)	4 (11)	1 (4)
Telangiectasic	4 (8)	3 (7)	3 (9)	1 (4)

NOTE: Figures indicate the number of patients. Values in brackets indicate percent out of total patients in the group.

MAb (2 μg/mL), or the 2 combined MAb, or the MOPC-21 control MAb (1 μg/mL), or BMS536924 (BMS; 0.05–0.10–0.50–1.00–5.00 μmol/L). Cell growth was evaluated by trypan blue at 72 and 144 h. Growth curves were repeated twice, in duplicate. *b) siRNA blocking strategy.* Specific gene silencing effect was evaluated by siRNA technology associated with pipette-type electroporation. Cells were trypsinized at semiconfluence and counted by trypan blue. Fifteen microliters of cell suspension containing 300,000 cells and 2 pmol of specific or control siRNA were transferred into a 1-mm cuvette, and an electrical field was applied to induce siRNA cellular internalization (MicroPorator MP-100; Digital BioTechnology). For the assay with anti–IR-siRNA and anti–IGFIR-siRNA, after electroporation, Saos-2 cells were transferred into 2 mL of complete growth medium and seeded in 6-well plates (150,000 cells per well). After 4 d, cells were counted by trypan blue and lysated. Protein lysates were subjected to immunoblot analysis for IGFIR, IR, and tubulin (anti–α-tubulin B7 MAb). Growth assay was repeated twice in duplicate. For the assays with anti–IGF-II-siRNA, after electroporation, MG-63 were transferred into 2 mL of medium with 0.5% FCS, and seeded in 6-well plates (600,000 cells per well). After 4 d, cells were counted by trypan blue and lysated. Five micrograms of total proteins were used for the IGF-II ELISA assay. The growth curve and IGF-II assay were repeated twice in duplicate.

Blocking strategies on tumorigenesis. Anchorage-independent growth was evaluated after exposure to MAb against IGFIR and/or IGF-II. Saos-2 and MG-63 were exposed to αIR-3 MAb (1 μg/mL), S1F2 MAb (2 μg/mL), both, or to control MAb (1 μg/mL) for 3 d, and then seeded (3300 cells/plate) in 0.33% agarose with a 0.5% agarose underlay (SeaPlaque Agarose) in complete medium. After incubation at 37°C for 5 to 6 d, colonies of >125 μm were counted. Results were expressed as percentages. The experiment was performed in duplicate and repeated twice.

Statistical analysis. Statistics was performed with the StatViewTM 5.0.1 software (SAS Institute). Due to the low number of observations, data were considered as not normally distributed, and nonparametric tests were used. The Mann-Whitney U test was used for the difference between groups, the Wilcoxon Rank test was used for the difference of paired values in patients before and after treatment, and the Spearman rank test was used for the correlation between continuous variables. To evaluate the prognostic performance of IGF-I, IGF-II, and IGFBP-3, the 95th percentile of control group was used as a threshold value in Kaplan-Meier plots and in the log-rank test.

Results

IGFs and IGFBP-3 serum levels. IGF-I serum levels of OS patients (n = 45) were significantly lower than those of age-matched controls (n = 17; median, 168.0 ng/mL; range, 50.0–452.0 ng/mL versus 303.0 ng/mL; range, 92.0–559.0 ng/mL, respectively; P = 0.0005). In contrast, IGF-II serum levels were significantly higher (median, 949.0 ng/mL; range, 402.0–1786.0 ng/mL versus 749.0 ng/mL; range, 590.0–979.0 ng/mL; P = 0.0191; Fig. 1*A*). No correlation was found between IGF-I and IGF-II levels. IGFBP-3 serum levels were significantly lower (n = 40) than controls (n = 16; median, 3811.9 ng/mL; range, 1746.6–5256.8 ng/mL versus 4342.0 ng/mL; range, 3276.6–5293.1 ng/mL; P = 0.0203; Fig. 1*A*). As expected, serum levels of IGFBP-3 were positively related both to IGF-I (P < 0.0001; r = 0.561) and IGF-II (P = 0.0033; r = 0.396) values.

In a subgroup of 9 unrelapsed patients, in which blood samples were obtained both at diagnosis and after 12 months, at the completion of surgical and chemotherapeutic treatments, both IGF-I and IGF-II levels turned to normal values (P = 0.021 and 0.007 versus values at presentation, respectively; Fig. 1*B*).

Serum IGF-I, IGF-II, and IGFBP-3 levels were examined in relation to event-free survival. Increased IGF-II serum levels were significantly associated with a decreased probability of remaining free of disease (P = 0.0372), which was 50% in patients with high IGF-II levels (above 944 ng/mL) and 84% in patients with normal IGF-II levels (Fig. 1*C*). In contrast, both IGF-I and IGFBP-3 serum levels were not associated with an adverse outcome.

IGFs, IR, IGFIR, and HR expression in OS tissue. In 23 OS tissue specimens, we measured IGFIR, IR, and HR protein content. Receptor content was considered positive if equal or above 0.3 ng/100 μg protein. IGFIR was positive in 20 of 23, IR in 21 of 23, and HR in 23 of 23. Interestingly, the HR exceeded IGFIR in 19 of 23 cases (Table 2; Fig. 1*D, top*). There was a significant correlation between IGFIR and HR expression (P = 0.0053; r = 0.594) but not between IR and HR.

The analysis of the expression of the two IR isoforms by RT-PCR indicated that IR-A was expressed in 19 of 19 cases, whereas IR-B was expressed only in 6 of 19 OS (Table 2; Fig. 1*D, bottom*).

IGF-II mRNA was abundantly present in 17 of 19 cases, and IGF-I mRNA in 14 of 19 cases (Table 2). IR-A was always higher than IR-B.

Taken together, these data indicate that human OS produce large amounts of IGF-II, to a greater extent than IGF-I, and that they also express the IR-A and HR rather than IGFIR.

Effects of IGFs and insulin on OS cell proliferation. The role of IGF-II, IR-A, and HR in OS was further investigated in two cell lines. In Saos-2 only IR-A was expressed, whereas in MG-63 both isoforms were expressed, with IR-B prevalence (Fig. 2*A*). In Saos-2, IGFIR was 5.7 ng, IR was 1.5 ng, and HR was 7.2 ng/0.1 mg total protein, whereas in MG-63, IGFIR was 0.9 ng, IR was 2.6 ng, and HR was 2.2 ng/0.1 mg. In both cell lines, the amount of HR was higher than IGFIR. We also quantified the intracellular content for IGF-I and IGF-II. Saos-2 expressed low levels of IGF-I (0.1 ng/0.1 mg protein), whereas MG-63 did not express detectable amount of IGF-I. Adversely, MG-63 had a high content of IGF-II (29.3 ng/0.1 mg protein) that was not detectable in Saos-2. In Saos-2 that secrete low level of IGFs, in serum-free conditions, exogenously added IGF-I and IGF-II induced a significant increase of proliferation compared with untreated cells (P = 0.0495 and 0.0433, respectively), whereas insulin had no effect (Fig. 2*B*).

The intracellular pathway activation of the IGF system was evaluated by immunoblotting. The presence of a mild phosphorylation of IR, ERK, and IRS-1 in unstimulated MG-63 is consistent with the presence of a strong autocrine circuit for IGF-II (Fig. 2*C*). In Saos-2, the phosphorylation of IGFIR and IR, and a time-dependent phosphorylation of ERK and IRS-1, was observed after

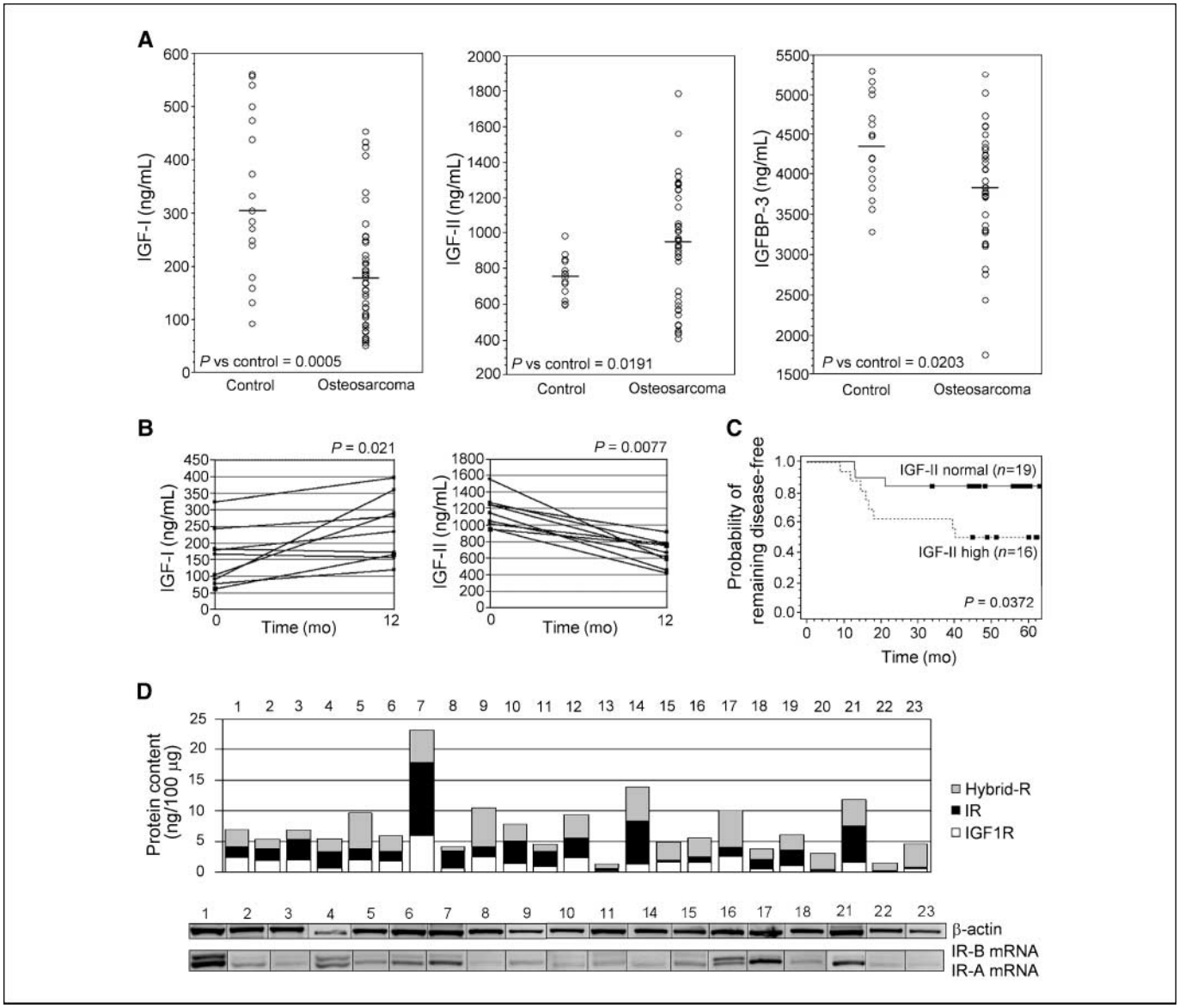

Figure 1. Serum levels of IGF-I and IGF-II, and expression of their receptors in OS tissue samples. *A,* IGF-I, IGF-II, and IGFBP-3 serum levels in patients versus control subjects. *Black lines,* median values. *B,* IGF-I and IGF-II serum level trend in patients at diagnosis and 12 mo since diagnosis (after treatment). *C,* probability of event-free survival in nonmetastatic patients with a single bone lesion, with high and normal IGF-II serum levels. *D,* graph representation of protein content for IGFIR, IR, and HR in tissue specimens (*top*). *Bottom,* gel electrophoresis analysis of IR-A and IR-B cDNA from tissues. The primers used annealed before and after the exon 11. IR-A is without exon 11 (630 bp), IR-B is with exon 11 (636 bp). Representative experiment.

Table 2. mRNA analysis and protein expression of IGF-I, IGF-II, IR (total and isoforms), IGFIR, and Hybrid-Rs in 23 OS tissue specimens

	mRNA*				Receptor protein †		
Case no.	IGF-I	IGF-II	IR-A	IR-B	IGFIR (ng/0.1 mg)	IR (ng/0.1 mg)	Hybrid-Rs (ng/0.1 mg)
1	+	++	++++	+++	2.4	1.8	2.8
2	+	+++	+	−/+	1.9	1.9	1.6
3	++	+++	+	−/+	2.0	3.4	1.5
4	+++	+++	+++	+++	0.7	2.6	2.2
5	−	+	++	+	2.0	1.8	5.9
6	+	++	++	+	1.8	1.6	2.5
7	+	++	+++	+	5.9	12.0	5.3
8	−	−	+	−	0.7	2.8	0.7
9	−	+	+	−	2.5	1.7	6.3
10	−	−	+	−/+	1.4	3.8	2.6
11	−	+	+	−/+	0.9	2.5	1.2
12	N.d.	N.d.	N.d.	N.d.	2.3	3.3	3.7
13	N.d.	N.d.	N.d.	N.d.	0.2	0.5	0.7
14	+	+	+	−	1.3	7.1	5.5
15	+++	+++	+	−/+	1.7	0.3	2.9
16	+	++	+++	+++	1.6	1.0	3.0
17	++	++	++++	−	2.6	1.5	6.0
18	++	++	++	−	0.5	1.7	1.6
19	N.d.	N.d.	N.d.	N.d.	1.1	2.6	2.4
20	N.d.	N.d.	N.d.	N.d.	0.2	0.3	2.6
21	++	++	+++	−	1.6	6.0	4.2
22	+	+	+	−	0.1	0.2	1.2
23	+	+	+	−	0.6	0.2	3.9
% of positive expression	14/19 (74%)	17/19 (89%)	19/19 (100%)	6/19 (32%)	20/23 (87%)	21/23 (96%)	23/23 (100%)

NOTE: mRNA and proteins were evaluated by RT-PCR and ELISA, respectively. Receptors content by ELISA analysis was considered positive if equal or above 0.3 ng/0.1 mg protein.

Abbreviation: N.d., not determined.

*Specific cDNA signal intensity on gel electrophoresis was evaluated by Quantity One Software (Bio-Rad) and related to the intensity of the signal corresponding to β-actin product (relative intensity). Grading was assigned depending on the relative intensity.

† Protein content is expresses as ng receptor/0.1 mg of cell protein.

both IGF-I and IGF-II stimulation. Insulin effect was observed only at 60 minutes for ERK, and at 15 to 60 minutes for IRS-1. In MG-63, a strong phosphorylation of IR, IGFIR, and a time-dependent phosphorylation of ERK and IRS-1 was induced by both IGF-I and IGF-II (Fig. 2*C*). A strong IR and IRS-1 activation was also observed after exposure to insulin.

Because previous studies had shown that IRS-1 is translocated to the nucleus when IGF-I–mediated nuclear translocation of β-catenin is required in actively growing cells (31, 32), we compared the ability of IGFs and insulin to induce IRS-1 nuclear translocation. IRS-1 was absent in the nucleus under basal conditions, but after exposure to IGF-I, IGF-II, or insulin, the number of cells with nuclear localization of IRS-1 significantly increased ($P = 0.0495$; Fig. 2*D, top*). This phenomenon was more evident in Saos-2, and seemed to be higher after IGF-II stimulation.

Effects of IGFIR and/or IR blocking strategies. We evaluated the antiproliferative effect of IGFIR blocking strategies, alone or in combination with IGF-II deprivation or IR inhibition. Cells were incubated with anti-IGFIR αIR-3 antibody and/or with anti–IGF-II S1F2 antibody. At 144 hours cell proliferation was significantly inhibited by α-IR3 ($P = 0.0209$ for Saos-2; $P = 0.0209$ for MG-63; Fig. 3*A*). A synergistic effect was obtained with a combined treatment with S1F2 and αIR-3 ($P = 0.0209$ for Saos-2; $P = 0.0209$ for MG-63). No significant inhibition effect was observed with S1F2 antibody alone. A significant inhibition was detected after treatment with the control antibody in MG-63 ($P = 0.0209$) but not in Saos-2.

Although our main interest was to elucidate the role of IR-A in OS, an efficient and specific anti–IR-A-siRNA is difficult to obtain because these differ only for the presence of exon 11. We therefore used an anti–IR-siRNA that cannot distinguish between the two isoforms. The growth inhibition effect of the anti–IR-siRNA compared with control anti–IR-siRNA was significant ($P = 0.0209$; Fig. 3*B, top*), as for anti–IGFIR-siRNA treatment compared with control anti–IGFIR-siRNA ($P = 0.0209$). The combined treatment with anti–IGFIR-siRNA and anti–IR-siRNA was more effective than treatments with IGFIR siRNA or IR siRNA treatment alone or no treatment ($P = 0.0209$ for all conditions; Fig. 3*B, top*). Moreover, the combined treatment with anti–IGFIR-siRNA and anti–IR-siRNA was significantly more effective than the combined two controls ($P = 0.0209$). Proliferation inhibition was paralleled by the specific expression impairment of the targeted protein by siRNA (Fig. 3*B, bottom*).

To evaluate the effect of impairment of the autocrine production of IGF-II in OS cells, we used an anti–IGF-II-siRNA only with

MG-63 because Saos-2 cells do not express IGF-II. Anti–IGF-II-siRNA treatment markedly decreased IGF-II protein content (1.3 ± 0.5 ng/100 μg for treated cells, 24.9 ± 2.1 ng/100 μg for untreated cells), whereas control siRNA had no effect (24.5 ± 2.9 ng/100 μg). In low-serum condition, the anti–IGF-II-siRNA also significantly inhibited cells proliferation (P = 0.0209; Fig. 3*C*).

We then evaluated the antitumorigenic effect of αIR-3 and S1F2 MAb (Fig. 3*D*). Consistently with the proliferation assay, inhibition of colony formation was significant for cells treated with αIR-3 and S1F2 MAb in combination (P = 0.0209 for both cell lines), and with αIR-3 MAb, or with S1F2 MAb for Saos-2 (P = 0.0209 in both cases), but not for MG-63. Treatment with the control MAb was ineffective

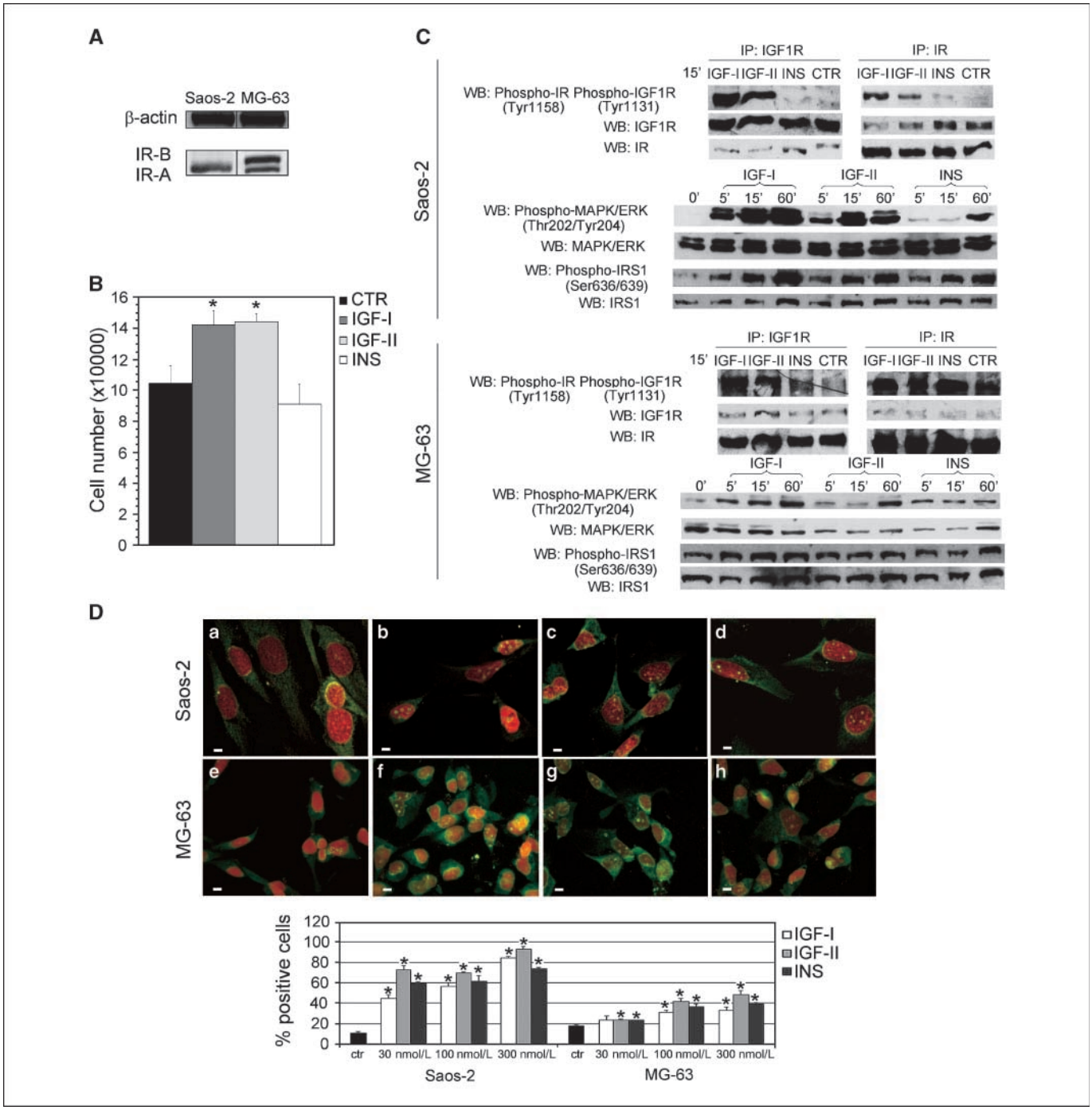

Figure 2. Induction of cell proliferation and IGF system activation by IGF-I, IGF-II, and insulin. *A,* IR-A and IR-B mRNA content in OS cell lines by gel electrophoresis. *B,* cell proliferation of Saos-2 exposed for 48 h to IGF-I, IGF-II, or insulin in serum-free condition. *Columns,* mean; *bars,* SE; *, P = 0.0495 for IGF-I; *, P = 0.0433 for IGF-II versus control (*CTR*). *C,* analysis of phosphorylation of immunoprecipitated IGFIR and IR, and of ERK1/2 and IRS-1 in total lysates of OS cells starved for 24 h, and then stimulated with IGF-I, IGF-II, or insulin for 15 min for immunoprecipitated samples, and for 5-15-60 min for total lysates. Representative experiment. *WB,* Western blotting; *IP,* immunoprecipitation. *D,* confocal representative images of IRS-1 localization in cells treated with IGF-I, IGF-II, or insulin (300 nmol/L; *top*). Saos-2 (*a–d*) and MG-63 (*e–f*) untreated (*a* and *e*), treated with IGF-I (*b* and *f*), with IGF-II (*c* and *g*), or with insulin (*d* and *h*). IRS-1 immunostained with FITC-polyclonal antibody (*green*). Nuclei counterstained with propidium iodide (*red*; *bars,* 10 μm). Overlaid images. *Bottom,* percentage of cells that showed IRS-1 nuclear translocation when treated with different concentrations of IGF-I, IGF-II, or insulin; *, P = 0.0495.

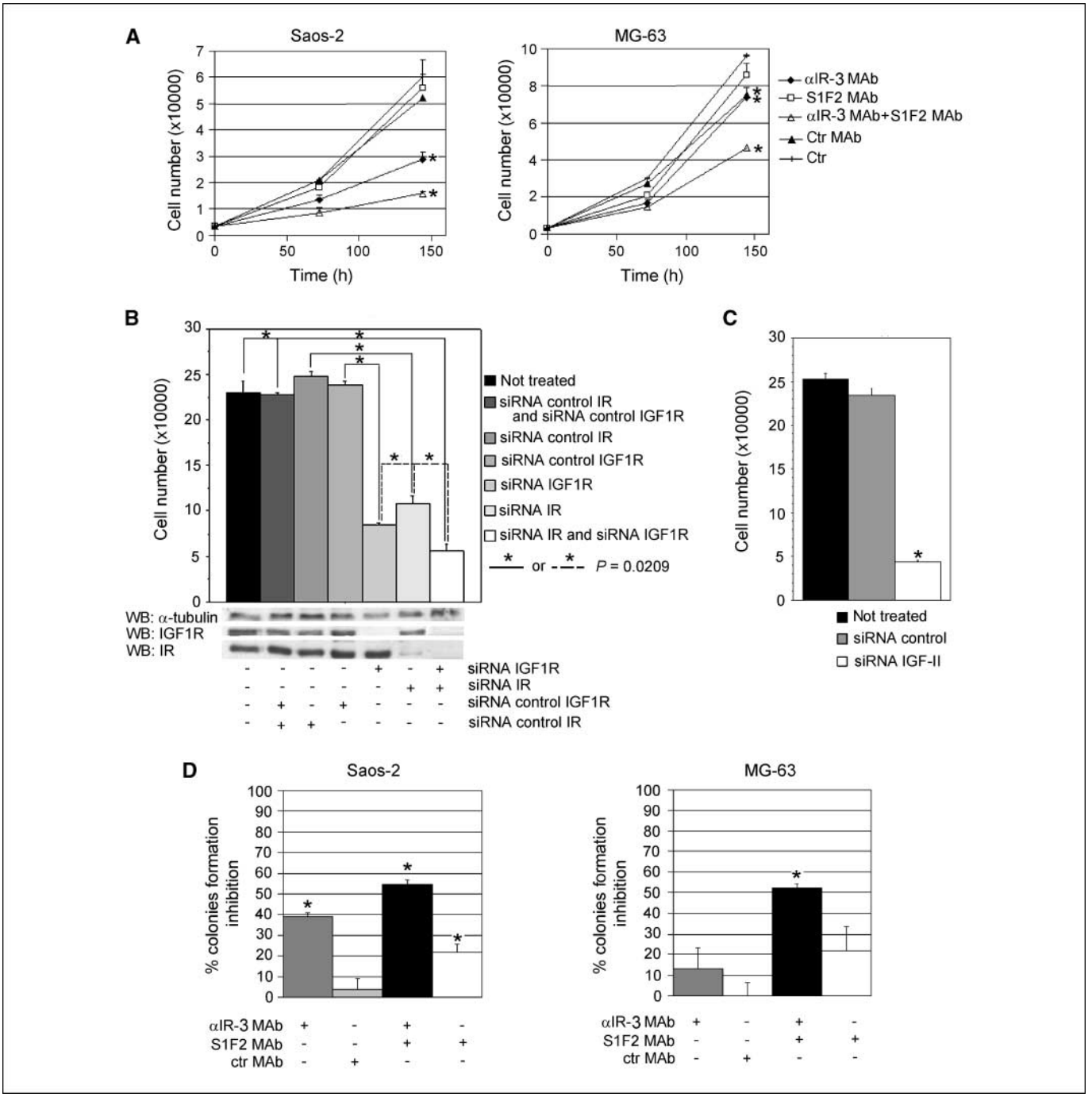

Figure 3. Effects of IR and/or IGFIR blocking strategies on cell growth and tumorigenesis. *A,* growth curves of cell incubated with anti–IGFIR αIR-3 MAb, anti–IGF-II S1F2 MAb, or with the two MAb combined. *Points,* mean; *bars,* SE, *, $P = 0.0209$ versus control at 144 h. *B,* effect on cell proliferation of IR and/or IGFIR inhibition by the siRNA technique. *Top,* cell number after 4 d of treatment with anti–IR-siRNA and/or anti–IGFIR-siRNA, or with their controls. *Columns,* mean; *bars,* SE; *, $P = 0.0209$. *Bottom,* Western blot analysis of IGFIR and IR content in cell lysates of cultures treated with different siRNA. Representative experiment. *C,* growth inhibition of MG63 treated with anti–IGF-II-siRNA after 4 d of culture in 0.5% serum-enriched medium; *columns,* mean; *bars,* SE; *, $P = 0.0209$. *D,* colony formation inhibition in soft agar cells pretreated for 3 d with αIR-3, S1F2, or the two MAb combined were plated in 0.33% agarose. Percentages of colony formation inhibition. *Columns,* mean; *bars,* SE; *, $P = 0.0209$ versus control.

in both cell lines. Moreover, combined treatment αIR-3 and S1F2 MAb seems to be always more effective than αIR-3 MAb or and S1F2 MAb alone. These results suggest that in cultured OS cells, both IR-A and HR may be considered as alternative receptors to IGFIR in inducing proliferation and tumorigenesis through IGF-II binding.

Effects of a IGFIR/IR-specific tyrosine kinase inhibitor on OS cells. Once, we showed the importance of IGFIR, IR, and HR in OS, we tested a tyrosine kinase specific inhibitor (33) for both IGFIR and IR as a candidate agent for OS treatment. BMS inhibited in a dose-dependent manner the proliferation and IGF signaling of

OS cells. A significant growth inhibition at 144 hours was observed at a ≥0.5 μmol/L dosage (P = 0.0209 for both cell lines) and at 0.1 mmol/L for MG-63 (P = 0.0304). In addition, in starved cells stimulated with IGF-II, increasing dosages of BMS-536924 reduced the phosphorylation of IGFIR/IR and of mitogen-activated protein kinase/ERK with a complete inhibition at 5.0 μmol/L (Fig. 4*B*).

Discussion

Under physiologic conditions, IGF-I produced by osteoblasts is an important regulator of bone cell metabolism and skeletal development under GH control (34). OS, which is likely to originate from a transformed osteoprogenitor cell (7), also secretes IGF-I (18), and this may be detected in the serum of OS patients. The IGF-I/IGFIR

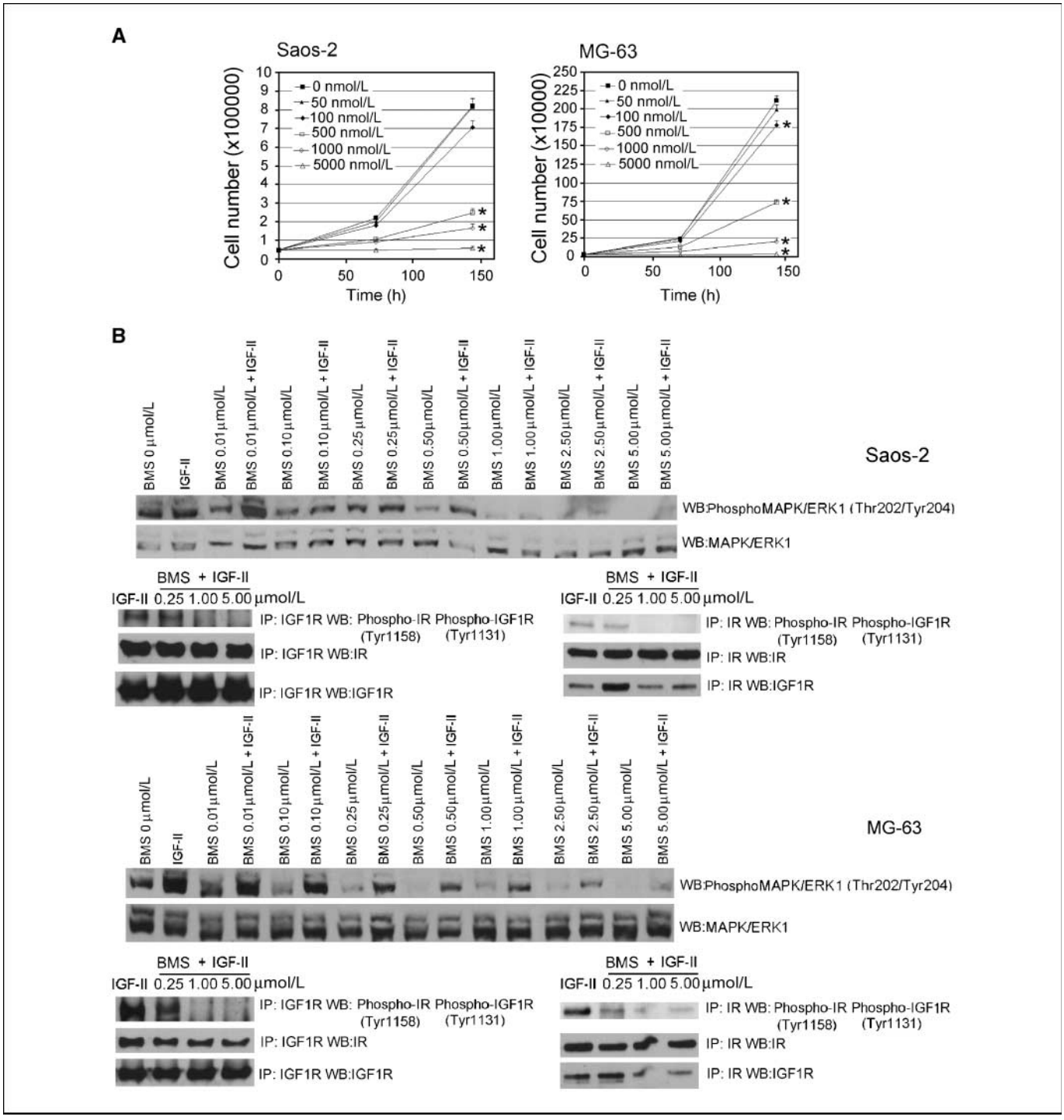

Figure 4. Effect of BMS-536924 on cell growth and on IGF-II–mediated signaling. *A,* growth curves with different concentrations of BMS536924 (*BMS*). *Points,* mean; *bars,* SE. At 144 h for dosages of ≥0.5 μmol/L, P = 0.0209 for both cell lines (*) and at 0.1 μmol/L, P = 0.0304 for MG-63 (*). *B,* Western blot analysis of IGF-II–induced phosphorylation of immunoprecipitated IGFIR, IR, and of ERK1/2 in total lysates of cells pretreated with increasing concentrations of BMS. Representative experiment.

autocrine circuit has long been considered as a key mechanism for the proliferation and survival of OS cells (11, 14, 16–18). However, circulating concentrations of IGF-I and its binding protein IGFBP-3 are not predictive of tumor incidence and/or clinical behavior (35), and therapeutic strategies that specifically block the binding of IGF-I to IGFIR have been only partially effective (5, 18). The lack of a significant therapeutic benefit suggests a redundancy within the IGF pathway. We therefore investigated whether other components of the IGF system are involved in OS pathogenesis.

In contrast to rodent bone cells, human bone cells produce less IGF-I than IGF-II, its cognate ligand (36–38). IGF-II has an important role during fetal development (20, 39), and during adult life, it is the most abundant growth factor stored in bones (37). Like IGF-I, IGF-II regulates bone cell metabolism and remodeling (40). In this study, for the first time, we report that IGF-II serum levels are significantly higher in OS patients compared with age-matched controls. In contrast to IGF-II, IGF-I, and IGFBP-3 are significantly lower than in controls. After tumor removal and chemotherapy, IGF levels return to normal values, suggesting that their variation is due to the presence of the tumor. These findings suggest that in OS patients the GH-IGF-I axis might be influenced by the increased serum levels of IGF-II produced by OS cells, as previously shown in sarcomas (41). Under this hypothesis, after tumor removal, IGF-II serum levels decrease and, as a consequence, GH secretion is no longer inhibited, leading to an increase of IGF-I serum levels. We did not evaluate the GH serum levels in this study due to the lack of multiple sequential sampling. Increased circulating IGF-II in OS patients might be related to the previously observed association between OS development and height, at least in growing individuals (10), as also suggested by an IGF-II role in prepubertal individual stature (42).

The relevance of IGF-II role in the biology of OS is also suggested by the significant correlation between high IGF-II levels and a poor prognosis in a homogeneous subset of patients. It is likely that increased IGF-II secreted by OS cells that express IGFIR (18) may activate an IGF-II/IGFIR autocrine loop that promotes cell proliferation and survival. In our series, we observed IGF-II mRNA in all OS tissue specimens. The IGFIR expression, however, was observed in most but not all OS cases. We, therefore, explored whether IGF-II could be active via another component of the IGF system, the IR isoform A, which results from alternative splicing of the IR gene (43) and plays an important role in embryonal and fetal development (25, 44, 45), and that is able to bind with high affinity to IGF-II (25). IR-A is overexpressed in several cancers (25, 27, 46, 47), including sarcomas (26, 48). In our series, IR-A was the predominant IR isoform in all cases. IR-A or IR-B heterodimers may combine with IGFIR heterodimers to form hybrid receptors that are often the most represented IGF system receptors. HR^A binds with high affinity and is activated by both IGF-I and IGF-II (27, 28). In our series, HR were always expressed and, in most cases, their expression level was significantly higher than that of IGFIR, indicating a relevant role of IGF-II in OS biology, and the existence of autocrine loops mediated by at least three different receptors (IR-A, HR^A, and IGFIR) that are alternatives to the less frequent IGFIR/IGF-II circuit.

The complex mechanism activated by IGF signaling in OS was confirmed in two OS cell lines that have an IGF-I/IGFIR autocrine circuit (18, 49). In Saos-2, we found the expression of IGFIR, IR-A, and HR^A, in MG-63 of IGFIR, IR-A, IR-B, and HR. We also found a strong autocrine circuit for IGF-II in MG-63, and a mild autocrine circuit for IGF-I in Saos-2. According to our data on OS patients, MG-63 cell line is more representative of clinical OS that secrete IGF-II, as indirectly shown. The crucial role of IGF-II autocrine circuit in OS cells was also shown by the use of an anti–IGF-II-siRNA that significantly inhibited MG-63 proliferation.

We then verified the effects of different ligands of the IGF system on cell proliferation and signaling. We found that IGF-II autocrine pathway in MG-63 is responsible for the phosphorylation of receptors under basal conditions, and that the expression pattern of receptors is very complex and the responsiveness to the different ligands is greatly redundant. In particular, there are three receptors (IGFIR, IR-A, and HR^A) for Saos-2, and six receptors (IGFIR, IR-A, IR-B, HR^A, HR^B, and Hybrids IR-A/IR-B) for MG-63, and the ligands (IGF-I, IGF-II, and insulin) can bind to and activate all these receptors. Therefore, it is hard to distinguish on which receptor each ligand is inducing the signaling cascade. We can only assume that in Saos-2, both IGF-I and IGF-II significantly promote cell growth, whereas only a slight effect is induced by insulin, and that the ligand-stimulation by either IGF-I, IGF-II, or insulin in both cell lines induce a strong phosphorylation and activation of receptors and of second messengers.

Considering the complexity of the IGF system in OS, blocking strategies specific for IGFIR or IR alone are unlikely to be successful, and in fact, selective IGFIR signaling inhibition was found to cause only limited effects (5, 18), whereas the use of an IGF-II sequestering MAb, combined with a IGFIR sequestering MAb, produced a stronger inhibition of both OS cell proliferation and tumorigenesis. In particular, IGF-II depletion alone was not effective in blocking tumor cell proliferation probably because of the presence of IGF-I. Similar results were obtained by selectively inhibiting IGFIR mRNA expression or IR mRNA expression or both by specific siRNA, or by selectively inhibiting with the tyrosine kinase inhibitor BMS-536924, which blocks both IGFIR and IR.

In conclusion, our data confirm the importance of the IGF signaling system in OS. In particular, IR-A and HR^A, both activated by IGF-II in addition to IGF-I, are involved. Our data suggest that cotargeting IGFIR and IR is likely to be more effective than targeting IGFIR alone.

Disclosure of Potential Conflicts of Interest

The authors have no conflicts of interest.

Acknowledgments

Received 7/10/2008; revised 11/25/2008; accepted 12/29/2008; published OnlineFirst 3/3/09.

Grant support: Ministry of Health (N. Baldini), Italian Association for Cancer Research (N. Baldini and R. Vigneri).

The costs of publication of this article were defrayed in part by the payment of page charges. This article must therefore be hereby marked *advertisement* in accordance with 18 U.S.C. Section 1734 solely to indicate this fact.

References

1. Bacci G, Ferrari S, Bertoni F, et al. Long-term outcome for patients with nonmetastatic osteosarcoma of the extremity treated at the Istituto Ortopedico Rizzoli according to the istituto ortopedico rizzoli/osteosarcoma-2 protocol: an updated report. J Clin Oncol 2000;18:4016–27.
2. Longhi A, Errani C, De Paolis M, Mercuri M, Bacci G. Primary bone osteosarcoma in the pediatric age: state of the art. Cancer Treat Rev 2006;32:423–36.
3. Lewis VO. What's new in musculoskeletal oncology. J Bone Joint Surg Am 2007;89:1399–407.

4. Baldini N, Scotlandi K, Barbanti-Bròdano G, et al. Expression of P-glycoprotein in high-grade osteosarcomas in relation to clinical outcome. N Engl J Med 1995; 333:1380–5.
5. Scotlandi K, Manara MC, Nicoletti G, et al. Antitumor activity of the insulin-like growth factor-I receptor kinase inhibitor NVP-AEW541 in musculoskeletal tumors. Cancer Res 2005;65:3868–76.
6. Patanè S, Avnet S, Coltella N, et al. MET overexpression turns human primary osteoblasts into osteosarcomas. Cancer Res 2006;66:4750–7.
7. Lee N, Smolarz AJ, Olson S, et al. A potential role for Dkk-1 in the pathogenesis of osteosarcoma predicts novel diagnostic and treatment strategies. Br J Cancer 2007;97:1552–9.
8. Fraumeni JF, Jr. Stature and malignant tumors of bone in childhood and adolescence. Cancer 1967;20:967–73.
9. Cotterill SJ, Wright CM, Pearce MS, Craft AW; UKCCSG/MRC Bone Tumour Working Group. Stature of young people with malignant bone tumors. Pediatr Blood Cancer 2004;42:59–63.
10. Longhi A, Pasini A, Cicognani A, et al. Height as a risk factor for osteosarcoma. J Pediatr Hematol Oncol 2005; 27:314–8.
11. Sekyi-Otu A, Bell RS, Ohashi C, Pollak M, Andrulis IL. Insulin-like growth factor 1 (IGF-1) receptors, IGF-1, and IGF-2 are expressed in primary human sarcomas. Cancer Res 1995;55:129–34.
12. Baserga R. The insulin-like growth factor I receptor: a key to tumor growth? Cancer Res 1995;55:249–52.
13. LeRoith D, Baserga R, Helman L, Roberts CT, Jr. Insulin-like growth factors and cancer. Ann Intern Med 1995;122:54–9.
14. Pollak MN, Polychronakos C, Richard M. Insulin-like growth factor I: a potent mitogen for human osteogenic sarcoma. J Natl Cancer Inst 1990;82:301–5.
15. Pollak M, Sem AW, Richard M, Tetenes E, Bell R. Inhibition of metastatic behavior of murine osteosarcoma by hypophysectomy. J Natl Cancer Inst 1992; 84:966–71.
16. Burrow S, Andrulis IL, Pollak M, Bell RS. Expression of insulin-like growth factor receptor, IGF-1, and IGF-2 in primary and metastatic osteosarcoma. J Surg Oncol 1998;69:21–7.
17. MacEwen EG, Pastor J, Kutzke J, et al. IGF-1 receptor contributes to the malignant phenotype in human and canine osteosarcoma. J Cell Biochem 2004;92:77–91.
18. Benini S, Baldini N, Manara MC, et al. Redundancy of autocrine loops in human osteosarcoma cells. Int J Cancer 1999;80:581–8.
19. Bautista CM, Baylink DJ, Mohan S. Isolation of a novel insulin-like growth factor (IGF) binding protein from human bone: a potential candidate for fixing IGF-II in human bone. Biochem Biophys Res Commun 1991; 176:756–63.
20. Baker J, Liu JP, Robertson EJ, Efstratiadis A. Role of insulin-like growth factors in embryonic and postnatal growth. Cell 1993;75:73–82.
21. Ohlaaon R, Nystrom A, Pfeifer-Ohlsson S, et al. IGF2 is parentally imprinted during human embryogenesis and in the Beckwith-Wiedemann sindrome. Nat Genet 1993;4:94–7.
22. Rainier S, Johnson LA, Dobry CJ, Ping AJ, Grundy PE, Feinberg AP. Relaxation of imprinted genes in human cancer. Nature 1993;362:747–9.
23. Ogawa O, Eccles MR, Szeto J, et al. Relaxation of insulin-like growth factor II gene imprinting implicated in Wilms' tumour. Nature 1993;362:749–51.
24. Ulaner GA, Vu TH, Li T, et al. Loss of imprinting of IGF2 and H19 in osteosarcoma is accompanied by reciprocal methylation changes of a CTCF-binding site. Hum Mol Genet 2003;12:535–49.
25. Frasca F, Pandini G, Scalia P, et al. Insulin receptor isoform A, a newly recognized, high-affinity insulin-like growth factor II receptor in fetal and cancer cells. Mol Cell Biol 1999;19:3278–88.
26. Sciacca L, Mineo R, Pandini G, Murabito A, Vigneri R, Belfiore A. In IGF-I receptor-deficient leiomyosarcoma cells autocrine IGF-II induces cell invasion and protection from apoptosis via the insulin receptor isoform A. Oncogene 2002;21:8240–50.
27. Pandini G, Vigneri R, Costantino A, et al. Insulin and insulin-like growth factor-I (IGF-I) receptor overexpression in breast cancers leads to insulin/IGF-I hybrid receptor overexpression: evidence for a second mechanism of IGF-I signaling. Clin Cancer Res 1999;5:1935–44.
28. Slaaby R, Schäffer L, Lautrup-Larsen I, et al. Hybrid receptors formed by insulin receptor (IR) and insulin-like growth factor I receptor (IGF1R) have low insulin and high IGF-1 affinity irrespective of the IR splice variant. J Biol Chem 2006;281:25869–74.
29. Pandini G, Medico E, Conte E, Sciacca L, Vigneri R, Belfiore A. Differential gene expression induced by insulin and insulin-like growth factor-II through the insulin receptor isoform A. J Biol Chem 2003;278: 42178–89.
30. Bacci G, Ferrari S, Mercuri M, et al. Neoadjuvant chemotherapy for extremity osteosarcoma-preliminary results of the Rizzoli's 4th study. Acta Oncol 1998;37: 41–8.
31. Sciacca L, Prisco M, Wu A, Belfiore A, Vigneri R, Baserga R. Signaling differences from the A and B isoforms of the insulin receptor (IR) in 32D cells in the presence or absence of IR substrate-1. Endocrinology 2003;144:2650–8.
32. Chen-J, Wu A, Sun H, et al. Functional significance of type 1 insulin-like growth factor-mediated nuclear translocation of the insulin receptor substrate-1 and β-catenin. J Biol Chem 2005;280:29912–20.
33. Wittman M, Carboni J, Attar R, et al. The discovery of a small molecule inhibitor of IGF-1R with broad spectrum *in vivo* activity. J Med Chem 2005;48:5639–43.
34. Rubin R, Baserga R. Insulin-like growth factor-I receptor. Its role in cell proliferation, apoptosis, and tumorigenicity. Lab Invest 1995;73:311–31.
35. Rodriguez-Galindo C, Poquette CA, Daw NC, Tan M, Meyer WH, Cleveland JL. Circulating concentrations of IGF-I and IGFBP-3 are not predictive of incidence or clinical behaviour of pediatric osteosarcoma. Med Pediatr Oncol 2001;36:605–11.
36. Middleton J, Arnott N, Walsh S, Beresford J. Osteoblasts and osteoclasts in adult human osteophyte tissue express the mRNAs for insulin-like growth factors I and II and the type 1 IGF receptor. Bone 1995;16: 287–93.
37. Conover CA. The role of Insulin-like growth factors and binding proteins in bone cell biology. In: Bilezikian JP, Raisz LG, Rodan GA, editors. Principles of Bone Biology. San Diego (CA): Academic Press; 1996. p. 607–18.
38. Mohan S, Jennings JC, Linkhart TA, Baylink DJ. Primary structure of human skeletal growth factor: homology with human insulin-like growth factor-II. Biochim Biophys Acta 1988;966:44–55.
39. Le Roith D. Seminars in medicine of the Beth Israel Deaconess Medical Center. Insulin-like growth factors. N Engl J Med 1997;336:633–40.
40. Mohan S, Baylink DJ. The role of Insulin-like growth factor I and II in the autocrine/paracrine regulation of bone-cell metabolism In: Novak JK, McMaster JH, editors. Frontiers of Osteosarcoma research. Seattle: Hoegrefe & Huber Publishers; 1993. p. 477–88.
41. Daughaday WH, Emanuele MA, Brooks MH, Barbato AL, Kapadia M, Rotwein P. Synthesis and secretion of insulin-like growth factor II by a leiomyosarcoma with associated hypoglycemia. N Engl J Med 1988;319: 1434–40.
42. Garrone S, Radetti G, Sidoti M, Bozzola M, Minuto F, Barreca A. Increased insulin-like growth factor (IGF)-II and IGF/IGF-binding protein ratio in prepubertal constitutionally tall children. J Clin Endocrinol Metab 2002;87:5455–60.
43. Moller DE, Yokota A, Caro JF, Flier JS. Tissue-specific expression of two alternatively spliced insulin receptor mRNAs in man. Mol Endocrinol 1989;3:1263–9.
44. Jonas HA, Newman JD, Harrison LC. An atypical insulin receptor with high affinity for insulin-like growth factors copurified with placental insulin receptors. Proc Natl Acad Sci USA 1986;83:4124–8.
45. Louvi A, Accili D, Efstratiadis A. Growth-promoting interaction of IGF-II with the insulin receptor during mouse embryonic development. Dev Biol 1997;189:33–48.
46. Vella V, Mineo R, Frasca F, et al. Interleukin-4 stimulates papillary thyroid cancer cell survival: implications in patients with thyroid cancer and concomitant Graves' disease. J Clin Endocrinol Metab 2002;87:45–254.
47. Denley A, Wallace JC, Cosgrove LJ, Forbes BE. The insulin receptor isoform exon 11- (IR-A) in cancer and other diseases: a review. Horm Metab Res 2003;35: 778–85.
48. Sun Y, Gao D, Liu Y, Huang J, Lessnick S, Tanaka S. IGF2 is critical for tumorigenesis by synovial sarcoma oncoprotein SYT-SSX1. Oncogene 2006;25:1042–52.
49. Kappel CC, Velez-Yanguas MC, Hirschfeld S, Helman LJ. Human osteosarcoma cell lines are dependent on insulin-like growth factor I for *in vitro* growth. Cancer Res 1994;54:2803–7.